Historical biogeography of the termite clade Rhinotermitinae (Blattodea: Isoptera)

Menglin Wang[1], Aleš Buček[1], Jan Šobotník[2], David Sillam-Dussès[3,4], Theodore A. Evans[5], Yves Roisin[6], Nathan Lo[7], Thomas Bourguignon[1,2]

[1]Okinawa Institute of Science & Technology Graduate University, 1919–1 Tancha, Onna-son, Okinawa, 904–0495, Japan

[2]Faculty of Forestry and Wood Sciences, Czech University of Life Sciences, Prague, Czech Republic

[3]Institut de Recherche pour le Développement – Sorbonne Universités, iEES-Paris, U 242, Bondy, France

[4]Université Paris 13 - Sorbonne Paris Cité, LEEC, EA 4443, Villetaneuse, France

[5]School of Biological Sciences, University of Western Australia, Perth WA 6009, Australia

[6]Evolutionary Biology and Ecology, Université Libre de Bruxelles, Belgium

[7]School of Biological Sciences, University of Sydney, Sydney, NSW, 2006, Australia

Author for correspondence: Thomas Bourguignon, e-mail: thomas.bourgui@gmail.com; thomas.bourguignon@oist.jp;

ABSTRACT

Termites are the principal decomposers in tropical and subtropical ecosystems around the world. Time-calibrated molecular phylogenies show that some lineages of Neoisoptera diversified during the Oligocene and Miocene, and acquired their pantropical distribution through transoceanic dispersal events, probably by rafting in wood. In this paper, we intend to resolve the historical biogeography of one of the earliest branching lineages of Neoisoptera, the Rhinotermitinae. We used the mitochondrial genomes of 27 species of Rhinotermitinae to build two robust time-calibrated phylogenetic trees that we used to reconstruct the ancestral distribution of the group. Our analyses support the monophyly of Rhinotermitinae and all genera of Rhinotermitinae. Our molecular clock trees provided time estimations that diverged by up to 15.6 million years depending on whether or not 3rd codon positions were included. Rhinotermitinae arose 50.4–64.6 Ma (41.7–74.5 Ma 95% HPD). We detected four disjunctions among biogeographic realms, the earliest of which occurred 41.0–56.6 Ma (33.0–65.8 Ma 95% HPD), and the latest of which occurred 20.3–34.2 Ma (15.9–40.4 Ma 95% HPD). These results show that the Rhinotermitinae acquired their distribution through a combination of transoceanic dispersals and dispersals across land bridges.

1. Introduction

Termites form a small insect group, comprising ~3000 species (Krishna et al., 2013). They primarily feed on wood or grass, but many species of Termitidae evolved to feed on decomposed substrates such as humus or soil (Abe, 1979). Termites reach their highest abundance in tropical and subtropical terrestrial ecosystems, where they are the principal decomposers of organic matter (Sugimoto et al., 2000).

Phylogenies based on mitochondrial genomes have shown that extant termites descend from a common ancestor that lived ~150 Ma (Bourguignon et al., 2015), and their distribution includes all of the continents other than Antarctica. Vicariance, through plate tectonics, and dispersal, across oceans and land bridges, are the two processes that can explain how organisms acquired their current distributions across continents. In the case of termites, plate tectonics might explain the global distribution of earliest branching lineages. However, the termite lineages that currently dominate warm ecosystems evolved only ~50 Ma (Bourguignon et al., 2015), and their distribution across the tropics is best explained by transoceanic and land bridge dispersals. Several tens of such dispersal events, each leading to termite lineages with modern representatives, took place during the Oligocene-Miocene period, 34–6 Ma (Bourguignon et al., 2016, 2017). This outstanding ability to disperse and colonise new continents is largely due to the wood feeding/nesting habit of many termite species, which favours dispersal by rafting across oceans in blown down trees and logs (Bourguignon et al., 2016, 2017).

Several recent studies have intended to resolve the historical biogeography of termites, primarily focusing on Neoisoptera (Bourguignon et al., 2016, 2017; Dedeine et al., 2016). However, one of the most basal lineages of Neoisoptera, the Rhinotermitinae, has been ignored so far. The Rhinotermitinae includes six genera (Krishna et al., 2013): *Acorhinotermes*,

Schedorhinotermes, *Rhinotermes*, *Dolichorhinotermes*, *Parrhinotermes*, and the doubtful *Macrorhinotermes*, a suspected synonym of *Schedorhinotermes* (Snyder, 1949). The group has living representatives in the Neotropical (13 species), Afrotropical (2 spp.), Oriental (35 spp.), New Guinean and Australian regions (16 spp.) (as defined by Holt et al., 2013), all of which feed on and live in dead wood (Krishna et al., 2013). Previous molecular phylogenetic trees unambiguously supported Rhinotermitinae as a monophyletic group, and time-calibrated trees estimated the last common ancestor of the group to be at 43 Ma (32–54 Ma 95% HPD) (Lo et al., 2004; Bourguignon et al., 2015). Since the divergence of Rhinotermitinae postdates the breakup of Gondwana, Rhinotermitinae are expected to have acquired their geographic distribution through dispersal, presumably via wood rafting across oceans, or via crossing of land bridges. In this study, we reconstructed the historical biogeography of Rhinotermitinae using phylogenetic trees inferred from the full mitochondrial genomes of 27 species. We used 12 termite fossils to infer a time-calibrated tree of Rhinotermitinae and to determine the timing of dispersal events.

2. Methods

2.1. Mitochondrial genome sequencing

We sequenced specimens from 23 termite species and used an additional four samples of Rhinotermitinae sequenced in previous studies (See Table S1). The outgroups comprise 71 non-Rhinotermitinae samples used by Bourguignon et al. (2015). Termite specimens were preserved in RNAlater® and stored at -80°C until DNA extraction. Whole genomic DNA was extracted from worker head and legs using the phenol-chlorophorm extraction procedure. The complete mitochondrial genome was amplified in two long-PCR reactions with the

TaKaRa LA Taq polymerase using primers previously designed for termites (See Table S2) (Bourguignon et al., 2015, 2016). The PCR conditions for the 10kb-fragment were as followed: initial denaturation at 95 °C for 1 min, followed by 30 cycles of 98°C for 10 s, 65°C for 30 s, and 68°C for 11 min, and a final extension at 72°C for 10 min. The PCR conditions for the 6kb-fragment were identical, except for the extension step during the 30 cycles, which was set to 7 min at 68°C instead of 11 min. We measured the concentration of both long-PCR fragments with the Qubit 3.0 fluorometer and mixed them in equimolar concentration. Sequencing of mixed long-PCR fragments was carried out through commercial service from BGI tech. Long-PCR fragments were fragmented and inserts of 300–500bp were multiplexed and 88bp-paired-end sequenced using Illumina HiSeq2000.

2.2. Mitochondrial genome assembly and annotation

We assembled 88 bp paired-end reads using the CLC suite of software, as previously described by Bourguignon et al. (2015). For polymorphic base pairs, we selected the most frequent base. The control region was systematically omitted from the final assembly because it comprises repeated regions that were difficult to assemble accurately with short reads.

We used the MITOS webserver to annotate the two ribosomal RNAs, 22 transfer RNAs, and 13 protein-coding genes (Bernt et al., 2013). In all cases, we ran MITOS using the invertebrate mitochondrial genetic code and default parameters. Annotated mitochondrial genomes were quality-checked against published termite mitochondrial genomes. Mitochondrial genomes were deposited in GenBank under accession numbers provided in Table S1.

2.3. Phylogenetic Analyses

We aligned each gene separately using the Muscle algorithm (Edgar, 2004), with default settings, implemented in MEGA 7.0.26 (Kumar et al., 2016). Ribosomal RNAs and transfer RNAs were aligned as DNA, and protein-coding genes as codons. Alignments were concatenated using FASconCAT (Kück and Meusemann, 2010).

We separated the dataset into five partitions (four partitions for analyses without third codon position): one partition for the combined tRNAs, one partition for the 12S and 16S, and one partition for each codon position of protein-coding genes. The same partition scheme was used for all phylogenetic elaborations. We reconstructed phylogenies using Bayesian and maximum likelihood methods. We examined each codon position of the protein-coding genes using the Xia's method in DAMBE (Xia and Lemey, 2009), and found no evidence of saturation at the third codon positions (NumOTU = 32, I_{SS} = 0.611, $I_{SS.c}$Asym = 0.809). Therefore, all phylogenetic analyses were performed twice, once with the third codon position included, and once with the third codon position excluded. We implemented Bayesian inferences in MrBayes version 3.2.3 (Ronquist et al., 2012), with unlinked partitions. All analyses were performed twice, once using a GTR+G+I model of nucleotide substitution, and once using a GTR+G model of nucleotide substitution. In all cases, we ran four MCMC chains (three hot and one cold) for 10^7 generations, and sampled the chain every 5,000 generations to estimate the posterior distribution. We excluded as burn-in the first 10^6 generations, as determined by Tracer version 1.5 (Rambaut and Drummond, 2007). We inferred maximum likelihood tree using RAxML v.8.2.4 (Stamatakis, 2014) and a GTRGAMMA model of nucleotide substitution. Branch supports were calculated using 1,000 bootstrap replicates.

2.4. Molecular dating

Molecular clock trees were computed in BEAST version 1.8.4 (Drummond and Rambaut, 2007). We used an uncorrelated lognormal relaxed clock to model rate variation among branches, with single model for each partition, allowing different relative rate. A Yule speciation model was used as tree prior. We used a GTR+G model of nucleotide substitution for each partition. MCMC chains were run for 10^8 generations, from which the first 10^7 generations were discarded as burn-in. The chain was sampled every 10,000 generations to estimate the posterior distribution. We used 12 fossils as minimum age constraints (See Table S3). We determined soft maximum bounds using phylogenetic bracketing (Ho and Phillips, 2009). Each calibration was implemented as exponential priors of node time. Each BEAST analysis, with and without third codon position, was executed thrice to ensure convergence of the chains.

2.5. Biogeographic Analyses

We reconstructed the geographic range of termites using the ace function implemented in the R package APE version 5.0 (Paradis et al., 2004). We used the Maximum Likelihood model described by Pagel (1994) and an equal-rates of transition. We also used the Bayesian Binary Method implemented in RASP version 4.0 (Yu et al. 2015), using both estimated and fixed model of state frequencies, and gamma and equal distribution rates across sites. Sampling locations were used to assign each tip to one biogeographic realm.

3. Results

3.1. Molecular phylogeny

Each of our analyses yielded identical tree topologies (Fig. 1), consistently supporting the monophyly of Rhinotermitinae. *Parrhinotermes* formed a monophyletic taxon, the sister group to all remaining Rhinotermitinae. *Schedorhinotermes* was also found to be

monophyletic, and formed the sister group of a clade composed of *Dolichorhinotermes* and *Rhinotermes*.

3.2. Divergence dating analyses

The analysis with third codon positions yielded consistently older age estimates (Supplementary Fig. S1), up to 15.6 My older than the analysis without third codon positions (Fig. 1). We provide the results of both analyses conjointly. The divergence time between *Parrhinotermes* and other Rhinotermitinae was estimated at 50.4–64.6 Ma (41.7–74.5 Ma 95% HPD). The most recent common ancestor of the examined *Parrhinotermes* species was estimated at 29.7–42.4 Ma (23.3–50.0 Ma 95% HPD). The clade composed of *Dolichorhinotermes* + *Rhinotermes* diverged from *Schedorhinotermes* 41.0–56.6 Ma (33.0–65.8 Ma 95% HPD), and the most recent common ancestor of all *Schedorhinotermes* species was dated to 26.5–41.3 Ma (21.1–48.8 Ma 95% HPD).

3.3. Biogeographic reconstruction

Our ancestral range reconstruction analyses all yielded similar results, and failed to precisely determine ancestral distributions. For simplicity, we present here the results of the maximum likelihood model (Figure 1), and the results obtained with the Bayesian binary model with estimated state frequencies and gamma-distributed rates across sites (Supplementary Fig. S2). Our analyses revealed four disjunctions among biogeographic realms. Significant uncertainties in the ancestral range reconstruction prevent us from drawing definitive conclusions on the direction of the dispersal. Within *Parrhinotermes*, the New Guinean *P. browni* diverged from Oriental *Parrhinotermes* at 29.7–42.4 Ma (23.3–50.0 Ma 95% HPD). The maximum likelihood model suggests that Oriental *Parrhinotermes* dispersed to the New

Guinean realm once, while the Bayesian binary models suggest that Oriental and New Guinea origins are equally probable. The Neotropical *Rhinotermes* and *Dolichorhinotermes* shared a last common ancestor at 24.0–35.7 Ma (16.8–45.3 Ma 95% HPD) and diverged from *Schedorhinotermes* 41.0–56.6 Ma (33.0–65.7 Ma 95% HPD). Our biogeographic reconstructions suggested that they dispersed to the Neotropical realm, possibly from the Oriental region. In contrast, our Bayesian binary models favour a Neotropical origin of the group, and a subsequent dispersal to the African realm. *Schedorhinotermes* consists of three lineages, each exclusively distributed in the African, Australian or Oriental realms, respectively. The African *Schedorhinotermes* diverged from other *Schedorhinotermes* 26.5–41.3 Ma (21.1-48.8 Ma 95% HPD), and the Oriental *Schedorhinotermes* diverged from the Australian *Schedorhinotermes* 20.3–34.2 Ma (15.9–40.4 Ma 95% HPD). The scenario favoured by the maximum likelihood model is an Oriental origin of *Schedorhinotermes* and a subsequent dispersal to Africa and Australia. The scenario favoured by the Bayesian binary models is an African origin of *Schedorhinotermes*, followed by one dispersal to the Oriental realm, from where it dispersed once more to the Australian realm.

4. Discussion

In this study, we conducted the most advanced phylogenetic analysis yet of the Rhinotermitinae. We found that the monophyletic *Parrhinotermes* forms the sister group of all other Rhinotermitinae, and that these two lineages diverged 50.4–64.6 Ma (41.7–74.5 Ma 95% HPD). Among the remaining Rhinotermitinae, *Schedorhinotermes* forms the sister group of *Dolichorhinotermes + Rhinotermes*, from which it diverged 41.0–56.6 Ma (33.0–65.8 Ma 95% HPD). The split between *Dolichorhinotermes* and *Rhinotermes* was estimated at 24.0–35.7 Ma (16.8–45.3 Ma 95% HPD). Two previous studies agreed with this branching pattern

(Austin et al., 2004; Bourguignon et al., 2015), while two other studies supported a sister relationship between *Schedorhinotermes* and *Parrhinotermes* (Lo et al., 2004; Inward et al., 2007). The position of *Parrhinotermes* as the earliest lineage in the tree, combined with the fact that it possesses a monomorphic soldier and worker castes, suggests that the soldier dimorphism of other Rhinotermitinae genera evolved once and was not lost since then, except perhaps in *Acorhinotermes* (Roisin, 2000).

Our molecular clock analysis with third codon positions yielded ages up to 15.6 My older than those without third codon positions. This large divergence is likely the result of the high substitution rate at the third codon position, which may have biased these estimations. Analyses with substitution-saturated sites are known to yield exaggerated age estimations, especially for recent divergences, which sometimes appear to be several times their actual age (Zheng et al., 2011). Therefore, our analysis without third codon positions is likely to be more realistic (Figure 1), and the actual divergence times within the Rhinotermitinae are probably similar to those of other termite lineages analysed to date (Bourguignon et al. 2016, 2017).

We found that the most recent common ancestor of modern Rhinotermitinae arose 50.4–64.6 Ma (41.7–74.5 Ma 95% HPD), i.e. after the final stage of the break-up of Pangaea. We therefore infer that they acquired their modern distribution through a series of dispersals over oceans through rafting in wood, and possibly through land bridges or aerial dispersal over water across short distances. Given the antiquity of the dispersal events, we can exclude human introduction as a mechanism of dispersal in Rhinotermitinae.

The *Gomphotherium* land bridge is believed to have created a terrestrial connection between Africa and Asia during the early Miocene ~18–20 Ma (Rögl, 1998). Both Oriental and African *Schedorhinotermes* clades are of similar age or younger than the *Gomphotherium* land bridge,

and therefore possibly dispersed through this route. In the case of the Australian *Schedorhinotermes,* the timing of the split between this lineage and the Oriental *Schedorhinotermes* is consistent with a crossing over Wallace's line, either through rafting, or aerial dispersal across the short distances that are thought to have existed between some pairs of islands respectively with an Oriental and Australian/Papua New Guinean origin. Similar scenarios have been proposed to explain the presence of geoscapheine and panesthiine burrowing cockroaches in Australia (Lo et al., 2016). However, in that case, Australian cockroach taxa were found to be nested within Asian lineages, whereas this pattern was not found for Australian and Asian *Schedorhinotermes*.

Following the scenario of an Oriental origin of Rhinotermitinae, ancestral rhinotermitines dispersed from there to South America, Africa, Australia and New Guinea. In the case of dispersal of *Rhinotermes* and *Dolichorhinotermes* from the Oriental realm to South America, this could be explained by oceanic rafting, as has been proposed for South American members of the Termitidae (Bourguignon et al., 2017). An alternative scenario is a Neotropical origin of Rhinotermitinae, following by one dispersal event to the Old World, from where it dispersed to Australia. Additional sampling, especially of the Neotropical *Acorhinotermes* and the Oriental *Macrorhinotermes* (should it not be a synonym of *Schedorhinotermes*) might help to distinguish among these alternative scenarios.

The four dispersal events we recorded among Rhinotermitinae lineages took place some time between the Eocene and Miocene periods, 56.6–6.0 Ma. Although our timeline is blurred by considerable uncertainties, the Rhinotermitinae might have dispersed worldwide through the Oligocene and Miocene periods, alongside the Termitidae and the subterranean termites (i.e. *Reticulitermes*, *Coptotermes*, and *Heterotermes*; Bourguignon et al., 2016, 2017; Dedeine et al., 2016). Under this scenario, Rhinotermitinae diversified and dispersed

worldwide following the opening of new ecological opportunities due to climate change. Modern Rhinotermitinae reached their highest abundance and diversity in tropical rainforests, one of the ecosystems which was significantly affected by the global cooling of the Eocene-Oligocene boundary (Morley, 2011).

Acknowledgements

References

Abe, T., 1979. Studies on the distribution and ecological role of termites in a lowland rain forest of west Malaysis. 2. Food and feeding habits of termites in Pasoh Forest Reserve. Jap. J. Ecol. 29, 121–135.

Austin, J.W., Szalanski, A.L., Cabrera, B.J., 2004. Phylogenetic analysis of the subterranean termite family Rhinotermitidae (Isoptera) by using the mitochondrial Cytochrome Oxidase II gene. Ann. Entomol. Soc. Am. 97, 548–555.

Bernt, M., Donath, A., Jühling, F., Externbrink, F., Florentz, C., Fritzsch, G., Pütz, J., Middendorf, M., Stadler, P.F., 2013. MITOS: improved *de novo* metazoan mitochondrial genome annotation. Mol. Phylogenet. Evol. 69, 313–319.

Bourguignon, T., Lo, N., Cameron, S.L., Šobotník, J., Hayashi, Y., Shigenobu, S., Watanabe, D., Roisin, Y., Miura, T., Evans, T.A., 2015. The evolutionary history of termites as inferred from 66 mitochondrial genomes. Mol. Biol. Evol. 32, 406–421.

Bourguignon, T., Lo, N., Šobotník, J., Sillam-Dussès, D., Roisin, Y., Evans, T.A., 2016. Oceanic

dispersal, vicariance and human introduction shaped the modern distribution of the

termites *Reticulitermes*, *Heterotermes* and *Coptotermes*. Proc. R. Soc. B Biol. Sci. 283,

20160179.

Bourguignon, T., Lo, N., Šobotník, J., Ho, S.Y.W., Iqbal, N., Coissac, E., Lee, M., Jendryka,

M.M., Sillam-Dussès, D., Křížková, B., Roisin, Y., Evans, T.A., 2017. Mitochondrial

phylogenomics resolves the global spread of higher termites, ecosystem engineers of the

tropics. Mol. Biol. Evol. 34, 589–597.

Dedeine, F., Dupont, S., Guyot, S., Matsuura, K., Wang, C., Habibpour, B., Bagnères, A.G.,

Mantovani, B., Luchetti, A., 2016. Historical biogeography of *Reticulitermes* termites

(Isoptera: Rhinotermitidae) inferred from analyses of mitochondrial and nuclear loci.

Mol. Phylogenet. Evol. 94, 778–790.

Drummond, A.J., Rambaut, A., 2007. BEAST: Bayesian evolutionary analysis by sampling

trees. BMC Evol. Biol. 7, 214.

Edgar, R.C., 2004. MUSCLE: A multiple sequence alignment method with reduced time and

space complexity. BMC Bioinformatics 5, 113.

Ho, S.Y.W., Phillips, M.J., 2009. Accounting for calibration uncertainty in phylogenetic

estimation of evolutionary divergence times. Syst. Biol. 58, 367–380.

Holt, B.G., Lessard, J.P., Borregaard, M.K., Fritz, S.A., Araújo, M.B., Dimitrov, D., Fabre, P.H.,

Graham, C.H., Graves, G.R., Jønsson, K.A., Nogués-Bravo, D., Wang, Z., Whittaker, R.J.,

Fjeldså, J., Rahbek, C., 2013. An update of Wallace's zoogeographic regions of the world.

Science 339, 74–78.

Inward, D.J.G., Vogler, A.P., Eggleton, P., 2007. A comprehensive phylogenetic analysis of termites (Isoptera) illuminates key aspects of their evolutionary biology. Mol. Phylogenet. Evol. 44, 953–967.

Krishna, K., Grimaldi, D.A., Krishna, V., Engel, M.S., 2013. Treatise on the Isoptera of the world: Vol 1, Introduction. Bull. Am. Mus. Nat. Hist. 377, 1989–2433.

Kück, P., Meusemann, K., 2010. FASconCAT: convenient handling of data matrices. Mol. Phylogenet. Evol. 56, 1115–1118.

Kumar, S., Stecher, G., Tamura, K., 2016. MEGA7: Molecular evolutionary genetics analysis version 7.0 for bigger datasets. Mol. Biol. Evol. 33, 1870–1874.

Lo, N., Kitade, O., Miura, T., Constantino, R., Matsumoto, T., 2004. Molecular phylogeny of the Rhinotermitidae. Insect. Soc. 51, 365–371.

Lo, N., Jun Tong, K., Rose, H.A., Ho, S.Y.W., Beninati, T., Low, D.L.T., Matsumoto, T., Maekawa, K., 2016. Multiple evolutionary origins of Australian soil-burrowing cockroaches driven by climate change in the Neogene. Proc. R. Soc. B Biol. Sci. 283, 20152869.

Morley, RJ., 2011. Cretaceous and Tertiary climate change and the past distribution of megathermal rainforests. In: Bush MB, Flenley J, Gosling WD, Morley RJ, editors. Tropical rainforest responses to climatic change. Chichester: Springer, Berlin, pp. 1–34.

Pagel, M., 1994. Detecting correlated evolution on phylogenies: a general method for the comparative analysis of discrete characters. Proc. R. Soc. B Biol. Sci. 255, 37–45.

Paradis, E., Claude, J., Strimmer, K., 2004. APE: Analyses of phylogenetics and evolution in R language. Bioinformatics 20, 289–290.

Rambaut, A., Drummond, A.J., 2007. Tracer. Available from: http://www.beast.bio.ed.ac.uk/Tracer

Rögl, F., 1998. Palaeogeographic considerations for mediterranean and paratethys seaways (Oligocene to Miocene). Ann. Naturhist. Mus. Wien 99A, 279–310.

Roisin, Y., 2000. Diversity and evolution of caste patterns. In: Abe T, Bignell DE, Higashi M, editors. Termites: evolution, sociality, symbioses, ecology. Dordrecht (The Netherlands): Kluwer Academic Publishers. pp. 95-119.

Ronquist, F., Teslenko, M., Mark, P. van der, Ayres, D.L., Darling, A., Höhna, S., Larget, B., Liu, L., Suchard, M.A., Huelsenbeck, J.P., 2012. MrBayes 3.2: efficient Bayesian phylogenetic inference and model choice across a large model space. Syst. Biol. 61, 539–542.

Snyder, E.A.E., 1949. Catalog of the termites (Isoptera) of the world. Smithson. Misc. Collect. 112, 1–490.

Stamatakis, A., 2014. RAxML version 8: a tool for phylogenetic analysis and post-analysis of large phylogenies. Bioinformatics 30, 1312–1313.

Sugimoto, A., Bignell, D.E., MacDonald, J.A., 2000. Global impact of termites on the carbon cycle and atmospheric trace gases, In: Abe T, Bignell DE, Higashi M, editors. Termites: evolution, sociality, symbioses, ecology. Dordrecht (The Netherlands): Kluwer Academic Publishers. pp. 409-435.

Xia, X., Lemey, P., 2009. Assessing substitution saturation with DAMBE. In: Lemey P, Salemi M, Vadamme A, editors. The phylogenetic handbook: a practical approach to DNA and protein phylogeny. United Kingdom: Cambridge University Press. pp. 615–630.

Yu, Y., Harris, A.J., Blair, C., He, X., 2015. RASP (Reconstruct Ancestral State in Phylogenies): a tool for historical biogeography. Mol. Phylogenet. Evol. 87, 46–49.

Zheng, Y., Peng, R., Kuro-O, M., Zeng, X., 2011. Exploring patterns and extent of bias in estimating divergence time from mitochondrial DNA sequence data in a particular lineage: A case study of salamanders (Order Caudata). Mol. Biol. Evol. 28, 2521–2535.
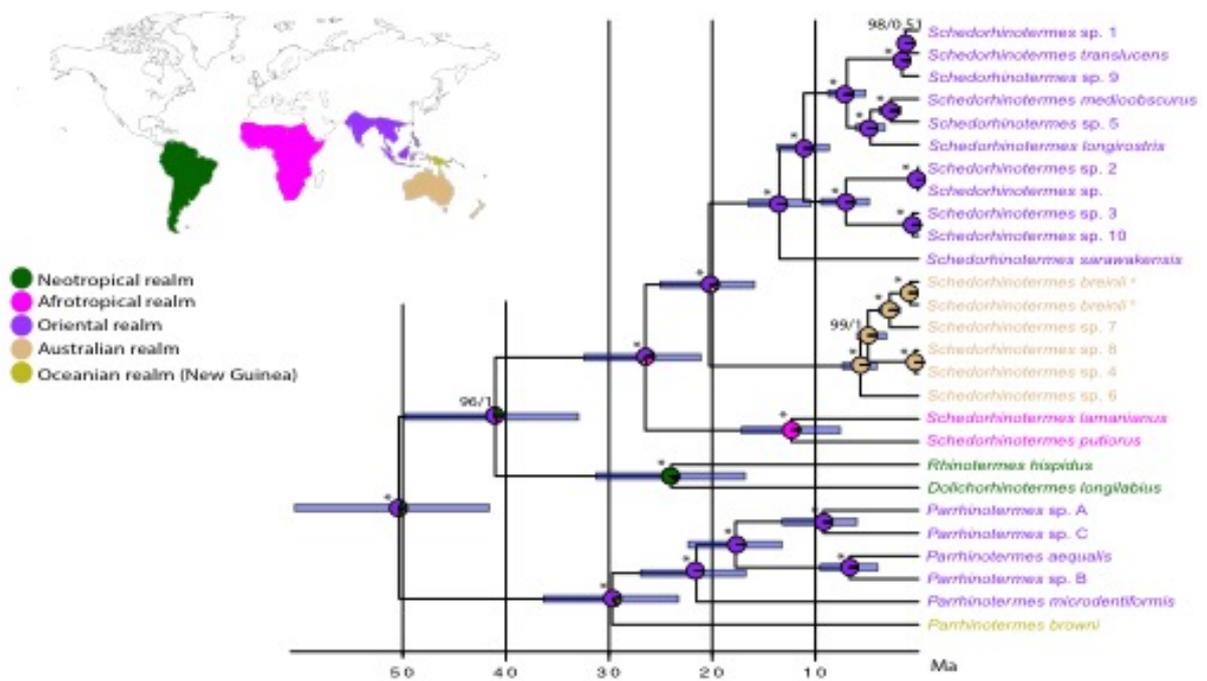
Fig. 1. Reconstruction of Rhinotermitinae lineage ancestral distributions, and estimates of divergence times within the group based on whole mitochondrial genomes, with third codon positions excluded. The map shows the biogeographic areas that were described in Holt et al. 2013. Phylogenetic tree was estimated in RAxML and Mrbayes. Branch support values indicate maximum-likelihood bootstrap support (percentage) and posterior probability in RaxML and MrBayes trees, respectively. Asterisks indicate 100% bootstrap support and 1.0 posterior probability. The bars at the nodes indicate the 95% HPD intervals for the ages. Pie charts indicate likelihoods of ancestral geographic range reconstructed with a maximum likelihood model.